



Development of small cyclic peptides targeting the CK2 α / β interface†

Eleanor L. Atkinson,^a Jessica Iegre,^a Claudio D'Amore,^b Paul Brear,^c Mauro Salvi,^{*b} Marko Hyvönen,^{*c} and David R. Spring^{*a}

Cite this: *Chem. Commun.*, 2022, 58, 4791

Received 4th February 2022,
Accepted 21st March 2022

DOI: 10.1039/d2cc00707j

rsc.li/chemcomm

In this work, an iterative cycle of enzymatic assays, X-ray crystallography, molecular modelling and cellular assays were used to develop a functionalisable chemical probe for the CK2 α / β PPI. The lead peptide, P8C9, successfully binds to CK2 α at the PPI site, is easily synthesisable and functionalisable, highly stable in serum and small enough to accommodate further optimisation.

CK2 is a ubiquitous and constitutively active protein kinase.¹ It has a heterotetrameric quaternary structure, consisting of two catalytic subunits (α or α') and two regulatory subunits (β).² The α / α' subunits carry out the phosphorylation of target proteins and peptide substrates, whereas the β subunits confer stability to the enzyme, control substrate specificity, and govern cellular localisation of the holoenzyme complex.³ In particular, CK2 β enhances the catalytic activity of CK2 α , as well as increasing its thermostability.⁴ CK2 β is also necessary for the protein shuttling of CK2 between intracellular compartments and, consequently, it controls the cellular location of the enzyme. Removal of CK2 β from the catalytic subunit prevents the formation of the holoenzyme, resulting in adverse effects upon substrate recognition, the stability of CK2 α , and its intracellular protein shuttling, all altering CK2's effect on the cell cycle.⁵

CK2 acts as an anti-apoptotic protein and is seen to be overexpressed in a wide variety of cancerous tumours.^{3,6–8} The absence of alternative pathways to compensate for CK2 down-regulation makes cancer cells particularly sensitive to CK2 inhibition.^{9–11} Promisingly, a first-in-class small molecule inhibitor, CX4945, has been designated as an orphan drug by FDA for the treatment of cholangiocarcinoma, and several clinical studies are ongoing for the treatment of different types of

tumours with this molecule, both alone and in combination therapies.¹²

There are multiple ways in which CK2 can be inhibited and the most widely researched of these methods is to target the ATP-binding site, which can be done with the aforementioned inhibitor CX4945.³ More recently, however, there has been a move towards targeting alternative sites on the protein.^{13–15} One such alternative method is *via* the inhibition of the protein–protein interaction (PPI) between the α and β subunits of CK2; the PPI interface is not as well conserved among other kinases as the ATP active site hence its inhibition is considered a more selective approach.² Preventing the formation of the CK2 holoenzyme would induce apoptosis by adjusting the substrate specificity and cellular location of the subunits, thus altering the intracellular environment.¹⁶

Peptides are good PPI modulators as their flexibility and size allows them to adapt to the large and shallow surfaces involved.¹⁷ This strategy has been applied to target CK2, and a handful of cyclic peptides are known to inhibit the CK2 PPI, most notably Pc, TAT-Pc and CAM7117.^{16,18,19} The most potent inhibitor, CAM7117, shows an improved K_d relative to Pc (200 nM vs. 1 μ M respectively), greater stability in human serum and antiproliferative activity in cancer cells.¹⁶ However, the synthesis of CAM7117 requires the use of an expensive unnatural amino acid, a non-commercially available staple, and three purification steps; thus the synthesis is expensive, slow and low yielding.¹⁶ Despite currently being the most potent peptide PPI inhibitor of CK2, its reduced activity in cellular assays and complex synthesis indicates that further work is required to develop a potent and selective peptide which inhibits CK2 in cells and is facily obtained.

We are building here on the CAM7117 work, developing novel conformationally-constrained peptides which are easily synthesised and with improved physicochemical properties to yield an enhanced chemical probe for the CK2 PPI.

Following iterative cycles of design, synthesis and testing, the sequence of CAM7117 was shortened. A lead sequence, able to bind to CK2 α and simultaneously present the side chains of

^a Yusuf Hamied Department of Chemistry, University of Cambridge, Lensfield Road, CB2 1EW, Cambridge, UK. E-mail: spring@ch.cam.ac.uk

^b Department of Biomedical Sciences, University of Padova, Padova, Italy. E-mail: mauro.salvi@unipd.it

^c Department of Biochemistry, University of Cambridge, Tennis Court Road, CB2 1GA, Cambridge, UK. E-mail: mh256@cam.ac.uk

† Electronic supplementary information (ESI) available. See DOI: 10.1039/d2cc00707j



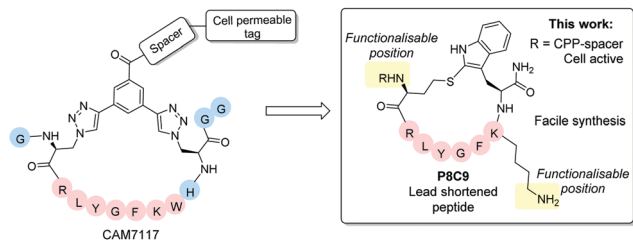


Fig. 1 Overview of the lead peptides developed in this work compared to the CK2 PPI inhibitor CAM7117.¹⁶ The shortened peptide **P8C9** is easily synthesisable, active in enzymatic assays and functionalisation with a cell penetrating peptide (CPP)-spacer yields good cellular activity. Blue spheres = residues removed from CAM7117 in **P8C9**.

two amino acids in a suitable position for constraining, was identified before being cyclised using a variety of constraints to obtain a peptide locked in its binding conformation (Fig. 1). The binding mode of the lead cyclic peptide was investigated using X-ray crystallography of the ligand in complex with CK2 α . This peptide was then tested in cellular assays to evaluate its ability to reduce cell viability.

Retention of good binding affinity, combined with a reduction in the molecular weight, resulted in an increase in the ligand efficiency (LE) of the peptide, whilst addition of a cell penetrating tag provided good cellular activity, with all peptides being facile to synthesise in two steps without needing synthetic staples and complex unnatural amino acids.

Analysis of the X-ray crystal structure of unfunctionalised CAM7117 (sequence GX_{C1}RLYGFKWHX_{C1}GG) bound to CK2 α (PDB: 6Q4Q) strongly suggests that the key binding interactions between the peptide and CK2 α are focused within the cyclic portions of the peptide.¹⁶ Therefore, shortened peptides using the central binding sequence of CAM7117 (RLYGFKWH) were chosen to investigate which residues could be used for cyclising the peptide into its binding conformation.

Molecular modelling suggested that only two positions (other than those used in CAM7117) could be used for constraining the central peptide sequence, RLYGFKWH: Trp and Aza-alanine (Aza) residues (Fig. S1, ESI[†]). Cyclisation of the Trp and Aza residues would allow for even greater shortening of the peptide sequence than simple removal of the terminal Gly residues. Additionally, the distance between the α -carbons of the Trp and Aza residues (7.5 Å) is shorter than between the two Aza residues in CAM7117 (11.6 Å) meaning that the size of the constraint used could also be reduced (Fig. S1, ESI[†]).

Before proceeding to the synthesis of constrained peptides, a series of linear peptides was synthesised based upon the central sequence of CAM7117 (RLYGFKWH) to determine which amino acids could be removed without compromising activity.

The peptide sequences initially synthesised are outlined in Table 1 alongside that of unfunctionalised CAM7117 (**P₊**, CAM7117 without the tri-Arg tag and spacer). Additionally, a reverse-sequence peptide, **P₋** (HWKFGYLR), was synthesised for use as a negative control in subsequent assays.

Table 1 Linear peptide sequences synthesised and the number of residues they contain. All peptides feature an amide at the C-terminus and are acetyl-capped at the N-terminus. X = Aza-alanine. X_{C1} = unfunctionalised constraint in CAM7117

Peptide	Sequence	No. of residues	IC ₅₀ (μM)
P1	RLYGFK	6	> 500
P2	LYGFKW	6	136.9 ± 25.8
P3	RLYGFKW	7	22.5 ± 2.4
P4	RLYGFKWH	8	16.7 ± 2.3
P₊	GX _{C1} RLYGFKWHX _{C1} GG	13	8.7 ± 4.2

To assess the ability of the synthesised linear peptides to displace a CK2 β -like fluorescent probe from CK2 α , a fluorescence polarisation (FP) assay was used (Table 1, ESI 1.3.2 and Fig. S2, ESI[†]). Comparison of the linear peptides indicates a large drop off in binding with the removal of the Arg (**P2** versus **P3**) and Trp residues (**P1** versus **P3**), suggesting that they both contribute positively to the activity of the peptide, with the removal of Trp resulting in a more profound loss of activity. The Ile to Trp mutation in CAM7117 resulted in a boost in potency (K_d = 150 nM, K_d = 460 nM for **P₊** and the corresponding peptide bearing Ile instead of Trp).¹⁶ Therefore, it is unsurprising that removal of the Trp residue resulted in a large loss in activity. Conversely, the His does not appear to be crucial to the binding ability of the peptide and, therefore, it was removed in the design of cyclic peptides.

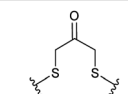
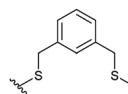
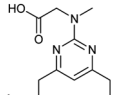
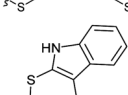
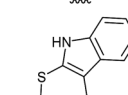
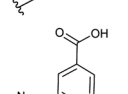
Combining the results of the molecular modelling, crystal structures and the FP of the linear peptides, the design of cyclic peptides was based upon the shortened peptide sequence RLYGFK, with two flanking residues for cyclisation at either end. Although the removal of Trp led to a loss in activity of the linear peptide, it was envisaged that its binding contribution could be compensated for by utilising an aromatic or hydrophobic staple, mimicking the properties of the Trp residue. For this purpose, the linear sequences CRLYGFKC (**P5**) and JRLYGFKX (**P6**) were used (J = propargylglycine, X = Aza-alanine) with a variety of constraints. Additionally, we considered keeping the Trp residue and stapling with Cys and homoCys (hC) residues using the linear sequences CRLYGKW (**P7**) and (hC)RLYGKW (**P8**) respectively with mild oxidative cyclisation conditions.²⁰ Furthermore, due to the small distance between the cyclising residues (7.9 Å), large constraints such as long alkyl chains and extended aromatic ring structures were ruled out. Instead, relatively small constraints were trialled (Table S1, ESI[†]).

The eight cyclic peptides synthesised were tested in an FP assay (Table 2 and ESI[†] Fig. S3). Both the triazole stapled peptides, **P6C2** and **P6C3**, showed negligible inhibition. **P5C4**, **P5C5**, **P5C7** and **P7C8** all showed reasonable activity, with IC₅₀ values between 15.6 and 54.6 μM. The methylene bridge-stapled peptide **P5C6** also showed distinct activity, although it was not quantifiable due to poor solubility.‡

Compared to **P₊**, **P8C9** showed a greater than 5 times increase in activity in our preliminary assay (Fig. S3–S5, ESI[†]), indicating that **P8C9** can efficiently engage CK2 α despite its reduced size. A comparison of the LEs (calculated as outlined in



Table 2 Structure of the active cyclic peptides tested, alongside their IC_{50} 's and ligand efficiencies (LEs). IC_{50} 's are reported \pm SEM. Peptide sequences: **P5CX** = $C_{CX}RLYGFKC_{CX}$, **P7C8** = $C_{C8}RLYGFKW_{C8}$, **P8C9** = $(hC)_{C9}RLYGFKW_{C9}$, **P₊** = $GXC_1RLYGFKWHX_{C1}GG$

Peptide	Constraint	IC_{50} (μ M)	LE
P5C4		54.6 ± 11.2	0.080
P5C5		28.9 ± 1.9	0.080
P5C7		40.0 ± 4.7	0.071
P7C8		15.6 ± 5.1	0.085
P8C9		1.7 ± 0.3	0.101
P₊		8.7 ± 4.2	0.057

eqn (S1), ESI[†]) of the novel peptides with that of **P₊** indicates that **P8C9** uses its structural features to target CK2 α the most effectively with a LE of 0.101 vs. 0.057 for **P₊** (Table 2).

Combination of the X-ray structures and IC_{50} values suggest that the homocysteine-cyclised peptide, **P8C9**, retains the binding conformation of the peptide more effectively than the cysteine-cyclised peptide, likely due to the flexibility provided by the extra carbon atom on the amino acid side chain (Fig. S6, ESI[†]). **P8C9** shows both an improved potency and an improved LE compared to **P₊** and, as such, represents a promising starting point for the development of potent and cell permeable CK2 PPI inhibitors.

The binding of **P8C9** to CK2 α was further assessed using ITC (Fig. S7, ESI[†]) and its K_d was found to be 750 nM.

The serum stability of **P8C9** was also analysed; it was found that **P8C9** was fully stable in serum over 24 h compared to the linear peptide **P8** which fully had degraded after 1 h (Fig. S8, ESI[†]). This was seen as a large improvement upon CAM7117 which is only 50% intact in serum after 24 h.¹⁶

X-ray crystallography was used to confirm the binding mode of **P8C9**. Comparison of the co-crystal structures of **P8C9** and **P₊** in complex with CK2 α indicates that the central binding sequence of the two peptides share the same binding conformation (Fig. 2c).

Functionalisation of **P8C9** would be desirable for the incorporation of cell penetrating tags, fluorescent dyes *etc.*; however, functionalisation through the staple is not facile due to the

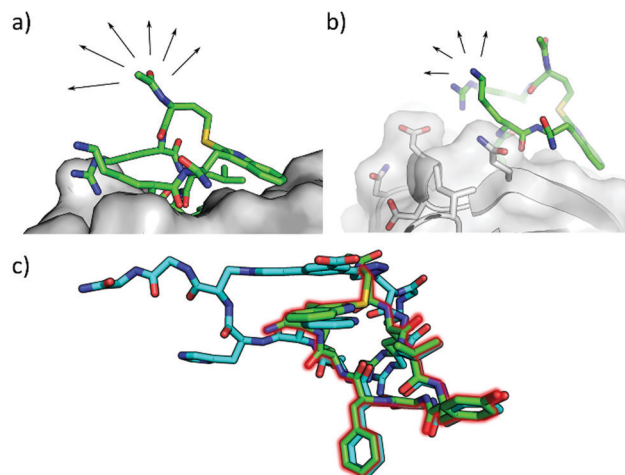


Fig. 2 X-ray co-crystal structure of **P8C9** in complex with CK2 α (PDB: 6YZH). (a and b) The N-terminus and Lys residue of **P8C9** are both solvent exposed making them good candidates as positions of functionalisation of the peptide. (c) Overlay of the crystal structures of **P8C9** and **P₊** in complex with CK2 α (PDB: 6Q4Q) highlighting that the central binding motif of the two peptides retain the same binding conformation.

one-component stapling used. The crystal structure of **P8C9** suggests that functionalisation of the peptide may be possible through the N-terminus or the Lys residue as both are solvent exposed (Fig. 2a and b). Indeed, functionalisation of the N-terminus of the peptide with a fatty acid and PEG chain only resulted in a minor decrease in binding affinity (K_d = 750 nM and 1.3 μ M for **P8C9** and **FA-P8C9** respectively Fig. S7, ESI[†]), as did functionalisation of the Lys residue with a PEG chain (K_d = 1.6 μ M for **P8C9**[PEG], Fig. S7, ESI[†]) indicating that the addition of large groups to either the N-terminus or the Lys residue of **P8C9** is likely to have little effect on its binding ability.

Finally, the effect of **P8C9** was evaluated in HeLa cells to determine if the peptide was able to reduce cell viability. Unfortunately, **P8C9** had no effect on cell viability (Fig. S10, ESI[†]). **FA-P8C9** was evaluated in cells and found to reduce the cell viability. However, **FA-PEG** alone was observed to cause some toxicity, and thus **FA-P8C9** was deemed to be causing partial non-specific toxicity (Fig. S11, ESI[†]).

Nevertheless, functionalisation of the N-terminus of **P8C9** with the known cell penetrating peptide sequence TAT (GRKKRRQRRRPPQ)²¹ joined to the peptide through a di-Ahx spacer, **TAT-P8C9**, resulted in a large reduction in cell viability (Fig. 3), as did analogous functionalisation with a tri-Arg tag (**R3-P8C9**, Fig. 3). No effect on cell viability was observed for the cell penetrating tag-spacer conjugates alone (**TAT-(Ahx)₂** and **R3-(Ahx)₂**, Fig. S13, ESI[†]). Thus, both **TAT-P8C9** and **R3-P8C9** represent promising CK2 modulating peptides for further investigation.

In conclusion, the structure of CAM7117 has been optimised to reduce its molecular weight whilst retaining good activity and its synthesis simplified. Various shortened cyclic peptides were synthesised and biologically evaluated. **P8C9** was found to



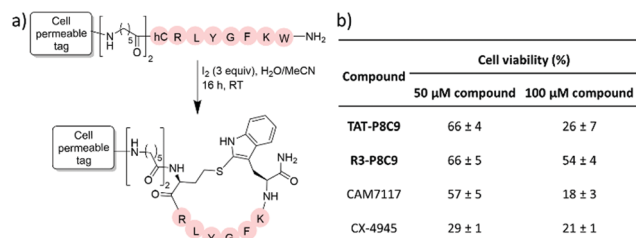


Fig. 3 (a) Structure of cell penetrating **P8C9** derivatives; CPP = TAT, **TAT-P8C9**; CPP = R3, **R3-P8C9**; hC = homocysteine. (b) Results of cell proliferation assay showing the percentage of viable cells remaining after treatment of HeLa cells with the specified compounds for 48 h. Average values are shown \pm standard deviation.

exhibit similarly high potency to CAM7117 in enzymatic assays, as well as retaining the same binding conformation and displaying an increased stability compared to CAM7117. Functionalisation of **P8C9** is possible through two positions on the peptide and incorporation of the cell penetrating peptides TAT and tri-Arg onto the N-terminus of the peptide provided peptides with good cellular toxicity. **P8C9** is the smallest peptide CK2 binder to date displaying high serum stability. Its facile synthesis makes it a much more attractive chemical probe than CAM7117 and its small structure leaves room for optimisation of both efficacy and pharmacokinetic properties.

Conflicts of interest

There are no conflicts to declare.

Notes and references

‡ Pleasingly, **P8C9** showed good activity ($1.7 \pm 0.3 \mu\text{M}$) and was used as a starting point for further optimisation.

§ Precipitation of **P8C9**[FA] occurred during ITC testing and thus, no K_d value could be obtained for the Lys-functionalised fatty acid derivative of **P8C9**.

- 1 C. Borgo, C. D'Amore, L. Cesaro, S. Sarno, L. A. Pinna, M. Ruzzene and M. Salvi, *Crit. Rev. Biochem. Mol. Biol.*, 2021, **56**, 321–359.
- 2 J. Iegre, E. L. Atkinson, P. Brear, B. M. Cooper, M. Hyvönen and D. R. Spring, *Org. Biomol. Chem.*, 2021, **19**, 4380–4396.
- 3 A. Siddiqui-Jain, D. Drygin, N. Streiner, P. Chua, F. Pierre, S. E. O'Brien, J. Bliesath, M. Omori, N. Huser, C. Ho, C. Proffitt, M. K. Schwaeb, D. M. Ryckman, W. G. Rice and K. Anderes, *Cancer Res.*, 2010, **70**, 10288–10298.
- 4 B. Guerra and O. G. Issinger, *Electrophoresis*, 1999, **20**, 391–408.
- 5 J. Hochscherf, D. Lindenblatt, M. Steinkrüger, E. Yoo, Ö. Ulucan, S. Herzig, O.-G. Issinger, V. Helms, C. Götz, I. Neundorff, K. Niefind and M. Pietsch, *Anal. Biochem.*, 2015, **468**, 4–14.
- 6 M. M. J. Chua, C. E. Ortega, A. Sheikh, M. Lee, H. Abdul-Rassoul, K. L. Hartshorn and I. Dominguez, *Pharmaceuticals*, 2017, **10**, 18.
- 7 J. H. Trembley, G. Wang, G. Unger, J. Slaton and K. Ahmed, *Cell. Mol. Life Sci.*, 2009, **66**, 1858–1867.
- 8 S. W. Strum, L. Gyenis and D. W. Litchfield, *Br. J. Cancer*, 2021, **2021**, 1–10.
- 9 P. Brear, A. North, J. Iegre, K. Hadje Georgiou, A. Lubin, L. Carro, W. Green, H. F. Sore, M. Hyvönen and D. R. Spring, *Bioorg. Med. Chem.*, 2018, **26**, 3016–3020.
- 10 K. A. Ahmad, G. Wang and K. Ahmed, *Mol. Cancer Res.*, 2006, **2**, 712–721.
- 11 M. Salvi, C. Borgo, L. A. Pinna and M. Ruzzene, *Cell Death Discovery*, 2021, **7**, 325.
- 12 Search of: CX-4945 – List Results – ClinicalTrials.gov, <https://clinicaltrials.gov/ct2/results?cond=&term=CX-4945&entry=&state=&city=&dist=>, (accessed 31 January 2022).
- 13 R. Prudent and C. Cochet, *Chem. Biol.*, 2009, **16**, 112–120.
- 14 P. Brear, C. De Fusco, K. Hadje Georgiou, N. J. Francis-Newton, C. J. Stubbs, H. F. Sore, A. R. Venkitaraman, C. Abell, D. R. Spring and M. Hyvönen, *Chem. Sci.*, 2016, **7**, 6839–6845.
- 15 J. Iegre, P. Brear, C. De Fusco, M. Yoshida, S. L. Mitchell, M. Rossmann, L. Carro, H. F. Sore, M. Hyvönen and D. R. Spring, *Chem. Sci.*, 2018, **9**, 3041–3049.
- 16 J. Iegre, P. Brear, D. J. Baker, Y. S. Tan, E. L. Atkinson, H. F. Sore, D. H. O'Donovan, C. S. Verma, M. Hyvönen and D. R. Spring, *Chem. Sci.*, 2019, **10**, 5056–5063.
- 17 L. Nevela and E. Giralt, *Chem. Commun.*, 2015, **51**, 3302–3315.
- 18 B. Laudet, C. Barette, V. Dulery, O. Renaudet, P. Dumy, A. Metz, R. Prudent, A. Deshiere, O. Dideberg, O. Filhol and C. Cochet, *Biochem. J.*, 2007, **408**, 363–373.
- 19 B. Bestgen, Z. Belaid-Choucair, T. Lomberget, M. Le Borgne, O. Filhol and C. Cochet, *Pharmaceuticals*, 2017, **10**, 16.
- 20 C. Puig Duran, F. Albericio Palomera and M. Gongora Benitez, *et al.*, WO/2019/030298, 2019.
- 21 A. D. Frankel and C. O. Pabo, *Cell*, 1988, **55**, 1189–1193.

